Chapter 1
Elementary Excitations of Isotope: Mixed Crystals

1.1 Introduction

The modern view of solid-state physics is based on the presentation of *elementary excitations*, having mass, quasiimpuls, electrical charge and so on (see, e.g. [17]). According to this presentation the elementary excitations of non-metallic materials are *electrons* (*holes*), *excitons* (*polaritons* [18]), and *phonons* [19]. The latter are the elementary excitations of the crystal lattice, the dynamics of which is described in harmonic approximation (see e.g. [20]). As is well known, the basis of such a view on solids is the multiparticle approach. In such a view, the quasiparticles of solids are ideal gas, which describe the behavior of the system, e.g. noninteracting electrons. We should include such approach to consider the theory of elementary excitations as a suitable model for the application of the common methods of quantum mechanics for the solution of solid-state physics tasks. In this part of our review we briefly consider not only the manifestations of the isotope effect in different solids, but also bring the new accurate results, showing the quantitative changes of different characteristics of phonons and electrons (excitons) in solids with isotopical substitution (see, also [21]). The isotopic effect becomes more pronounced when we deal with solids. For example, on substitution of H with D the change in energy of the electron transition in solid state (e.g. LiH) is two orders of magnitude larger than in atomic hydrogen (see, e.g. [22]). The use of elementary excitations to describe the complicated motion of many particles has turned out to be an extraordinarily useful device in contemporary physics, and it is the view of a solid which we describe in this part of the book.

The basic Hamiltonian of our solid model is of the form [21]

$$\mathrm{H} = \mathrm{H}_{\mathrm{ion}} + \mathrm{H}_{\mathrm{electron}} + \mathrm{H}_{\mathrm{electron-ion}} \tag{1.1}$$

where

$$\mathrm{H}_{\mathrm{ion}} = \sum_i \frac{p_i^2}{2m} + \frac{1}{2}\sum_{i \neq j} V(R_i - R_j), \tag{1.2}$$

V. G. Plekhanov, *Isotope Low-Dimensional Structures*, SpringerBriefs in Physics,
DOI: 10.1007/978-3-642-28613-1_1, © The Author(s) 2012

$$\mathrm{H_{electron}} = \sum_i \frac{p_i^2}{2m} + \frac{1}{2}\sum_{i\neq j} \frac{\mathrm{e}^2}{|r_i - r_j|}, \tag{1.3}$$

$$\mathrm{H_{electron-ion}} = \sum_{i,j} \mathrm{v}(\mathrm{r}_i - \mathrm{R}_j). \tag{1.4}$$

$\mathrm{H_{ion}}$ describes a collection of ions (of a single species) which interacts through a potential $\mathrm{V}(\mathrm{R}_i - \mathrm{R}_j)$ and which depends only on the distance between ions. By ion we mean a nucleus plus the closed-shell, or core, electrons, that is, those electrons that are essentially unchanged when the atoms are brought together to make a solid. $\mathrm{H_{electron}}$ presents the valence electrons (the electrons outside the last closed shell), which are assumed to interact via a *Coulomb* interaction. Finally, $\mathrm{H_{electron-ion}}$ describes the interaction between the electrons (excitons) and the ions, which is again assumed to be represented by a suitable chosen potential.

In adopting (1.1) as our basic Hamiltonian, we have already made a number of approximations in the treatment of a solid. Thus, in general the interaction between ions is not well—represented by a potential V(R), when the coupling between the closed-shell electrons on different ions begins to play an important role (see, e.g. [23, 24]). Again, in using a potential to represent electron–ion interaction, we have neglected the fact that the ions possess a structure (the core electrons); again, when the Pauli principle plays an important role in the interaction between the valence electrons, that interaction may no longer be represented by a simple potential. It is desirable to consider the validity of these approximations in detail (for details see, e.g. [24]). In general, one studies only selected parts of the Hamiltonian (1.1). Thus, for example, the band theory of solids is based upon the model Hamiltonian [23, 24]

$$\mathrm{H}_B = \sum_i \frac{p_i^2}{2m} + \sum_{i,j} \mathrm{v}(\mathrm{r}_i - \mathrm{R}_{j0}) + \mathrm{V_H}(\mathrm{r}_i), \tag{1.5}$$

where R_{j0} represents the fixed equilibrium positions of the ions and the potential V_H describes the (periodic) Hartree potential of the electrons. One studies the motion of a single electron in the periodic field of the ions and the Hartree potential, and takes the Pauli principle into account in the assignment of one-electron states. In so doing one neglects aspects other than the Hartree potential of the interaction between electrons. On the other hand, where one is primarily interested in understanding the interaction between electrons in metals, it is useful to consider only (1.3), replacing the effect of the ion cores by a uniform distribution of positive charge [25]. In this way one can approximate the role that electron interaction plays without having present the additional complications introduced by the periodic ion potential. Of course one wants finally to keep both the periodic ion potential and the electron interactions, and to include also the effects associated with departure of the ions from the equilibrium positions, since only in this way one does not arrive at a generally adequate description of the solid. Usually for the elementary excitations in solids

this is by first considering various different parts of the Hamiltonian (1.1) and then taking into account the remaining terms which act to couple different excitations.

1.2 Energy Band Structure

As mentioned above, the detailed study of the electronic band structure is the key to understand the behavior of electrons in solids, as well as their interaction with the lattice vibrations (phonons). The properties of a solid containing of the order of 10^{23} atoms/cm^3 are very complicated to predict. Several approaches to solve this problem were followed in the past providing a great amount of work in this field [23, 24]. For example, calculations of the band structure were performed using methods as $\vec{k} \cdot \vec{p}$, tight binding or LCAO, pseudo potentials, etc. (for details, see [23–26]).

Below, a simple basic frame to understand the electronic properties of crystal will be presented. It is not the author's purpose to give a detailed derivation of the fundamental equations governing the band structure, but to present the main ideas to understand the physical origin of the electronic band structure, phonon dispersion relations, and *electron–phonon interactions*, responsible, for instance, for the *Raman effect* (see also [20]).

First, we write the Hamiltonian describing a perfect crystal as [26]:

$$\mathrm{H} = \sum_i \frac{\mathrm{p}_i^2}{2\mathrm{m}_i} + \sum_j \frac{\mathrm{P}_j^2}{2\mathrm{M}_j} + \frac{1}{2}\bar{\sum_{j'j}} \frac{\mathrm{Z}_j \mathrm{Z}_{j'} \mathrm{e}^2}{4\pi\varepsilon_0 |\mathrm{R}_j - \mathrm{R}_{j'}|} - \sum_{ji} \frac{\mathrm{Z}_j \mathrm{e}^2}{4\pi\varepsilon_0 |\mathrm{r}_i - \mathrm{R}_j|} + \frac{1}{2}\sum_{ij} \frac{e^2}{4\pi\varepsilon_0 |\mathrm{r}_i - \mathrm{r}_j|}, \tag{1.6}$$

where r_i is the position of the ith electron, R_j the position of the jth nucleus, Z is the atomic number of the nucleus, p_i and P_j are the momentum operators of the electron and nucleus, respectively, e is the electronic charge, and $\bar{\sum}$ means that the summation is only over pairs of indices which are not identical. This many-particle Hamiltonian cannot be solved without a large list of simplifications:

1. **Valence electron approximation**. In the valence electron approximation we reduce the number of electrons, neglecting the core electrons [26]. We will take advantage of the fact that the core electrons are tightly bound to the nucleus forming the so-called ion core. Thus, the core electrons will no longer appear explicitly. For example, in the case of Si the electronic structure can be written as $1s^2 2s^2 2p^6 3s^2 3p^2$, where the 3s and 3p electrons are the only ones that hold are taken into account (see, also [27]).

2. **Born-Oppenheimer or adiabatic approximation [28]**. This approximation relies on the fact that ions are much heavier than electrons so they move much slowly.

Typically, the energy scales involved in the ionic motion is of the order of tens of meV, whereas the excitation energies for electrons is of the order of 1 eV. Converting these values into frequencies we obtain 10^{13} and $10^{15}\,\mathrm{s}^{-1}$ for lattice and electron vibrations, respectively. That is, the electronic frequencies are two orders of magnitude larger than the ionic vibrations, therefore the electrons 'see' the ions essentially stationary. Based on this we rewrite the Hamiltonian in Eq. (1.6) decoupling in part the movement of the electrons from that of the lattice as (see also [29]) was done above in Eq. (1.1). The purely electronic contribution to the Hamiltonian (1.1) $\mathrm{H}_{\mathrm{electron}}$ is the one responsible for the electronic excitation spectra in crystals, but still another approximation must be done in order to deal with the problem.

3. **Mean field approximation**. Taking only the electronic part in Eq. (1.1), we rewrite it as follows:

$$\mathrm{H}_e = \sum_i \frac{p_i^2}{2m_i} + \frac{1}{2}\sum_{i,i'}^{-} \frac{\mathrm{e}^2}{4\pi\varepsilon_0|\mathrm{r}_i - \mathrm{r}_{i'}|} - \sum_{i,j} \frac{\mathrm{Z}_j\mathrm{e}^2}{4\pi\varepsilon_0|\mathrm{r}_i - \mathrm{R}_{j0}|}, \tag{1.7}$$

where the first term is the kinetic energy of the electrons, the second is the *Coulomb* repulsion between electrons, and the last term is the Coulomb attraction between the nucleus in their equilibrium positions and the electrons. The mean field approximation replaces the Colombian terms in (1.7) by an average potential (see, e.g. [24]). The resulting Hamiltonian is given by:

$$\mathrm{H}_e = \sum_i \left[\frac{p_i^2}{2m_i} + \mathrm{V}(\mathrm{r}_i)\right] \Rightarrow \mathrm{H}_{1e} = \frac{p^2}{2m} + \mathrm{V}(\mathrm{r}), \tag{1.8}$$

where H_{1e} is the one-electron Hamiltonian and V(r) is the average potential. The first term in (1.8) is the free-electron Hamiltonian with plane waves as solutions. The energy spectrum is described by a parabolic dispersion relation as $\mathrm{E} = \frac{\hbar^2 k^2}{2m}$. The presence of the potential V(r) gives to the opening of the gap, and to the typical band structure of solid (see e.g. [26]). In order to obtain quantitative results, the one-electron potential V(r) is obtained, for example, using first principle calculations or semi-empirical methods.

The last step to obtain the band structure of solid is to take into account the rotational and translational symmetry of the crystalline structure. In this way, the wave functions that are solutions of (1.8) must have the same symmetry as the crystalline structure. By using group theory [30] it is possible to obtain these symmetries for each lattice structure and, thus, for the wave functions. Figure 1.1 shows the calculated band structure for Si in some highly symmetric directions of the *Brillouin zone*. As observed in this figure, the band structure of Si is indirect since the minimum transition energy is not at the zone center but in the $\Gamma \longrightarrow \mathrm{X}$.

The dependence of the band gap energy on *isotopic composition* has already been observed for insulators and lowest (indirect–direct) gap of different semiconductors (see also [22]). It has been shown to result primarily from the effect of the aver-

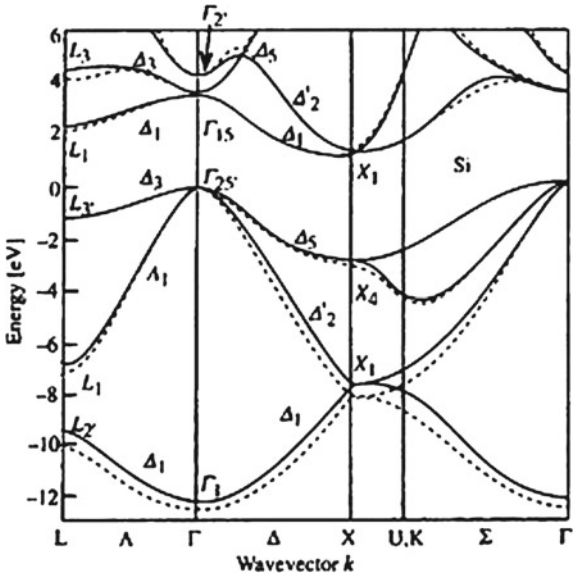

Fig. 1.1 Electronic band structure of Si calculated by pseudopotential technique. The *solid* and the *dotted lines* represent calculations with a nonlocal and a local pseudopotential, respectively (after [27])

age isotopic mass on the electron-phonon interaction (for details see below), with a smaller contribution from the change in lattice constant. This simplest approximation, in which crystals of mixed isotopic composition are treated as crystals of identical atoms having the average isotopic mass is referred to as *virtual crystal approximation* (*VCA*). Going beyond the VCA, in isotopically mixed crystals one would also expect local fluctuations in the band gap energy from statistical fluctuations in local isotopic composition within some effective volume, such as that of an exciton. Figure 91 of [31] shows the concentration dependence of the energy of interband transition E_g. As can be seen from this figure the VCA method cannot describe the observed experimental results. By now the change in E_g caused by isotopic substitution has been observed for many broad-gap and narrow-gap compounds (see Table 1.1). In Table 1.1 the variation of E_g and $\partial E_g / \partial M$ are shown at the isotopic effect. We should hihglight here that the most prominent isotope effect is observed in LiH crystal (see, also [22]).

1.3 Phonon States and Raman Spectra

The simplest kind of motion in solids is the vibration of atoms around the equilibrium point. The interaction of the crystal forming particles with one another at the move of one atom entangles neighbor atoms [20]. The analysis of this kind of motion shows that the elementary form of motion is the wave of the atom displacement. As is well known the quantization of the vibrations of the crystal lattice and after introduction of

Table 1.1 Values of the coefficients $\partial E_g/\partial M$ (meV) and energies of the band-to-band transitions E_g (eV) according to indicated references (after [22])

Substance	$\partial E_g/\partial M$ (meV)	E_g (eV)
$^{13}C \longrightarrow {}^{12}C$	14.6 [32]	5.4125 [32]
$^{7}LiH \longrightarrow {}^{7}LiD$	103 [33]	4.992 $\longrightarrow$ 5.095 [33]
$^{7}LiH \longrightarrow {}^{6}LiH$	12 [33]	4.980 [33]
$CsH \longrightarrow CsD$	60 [34]	4.440 [34]
$^{30}Si \longrightarrow {}^{28}Si$	2 [35]	3.652 [35]
$^{30}Si \longrightarrow {}^{28}Si$	2.09 [36]	1.166 [36]
$^{68}ZnO \rightarrow {}^{64}ZnO$	0.372 [37]	3.400 [37]
$Zn^{18}O \rightarrow Zn^{16}O$	3.533 [37]	3.400 [37]
$^{68}ZnO \rightarrow {}^{64}ZnO$	0.40 [38]	3.400 [37]
$Zn^{18}O \rightarrow Zn^{16}O$	3.20 [38]	3.400 [37]
$^{69}GaP \longrightarrow {}^{71}GaP$	0.19 [39]	2.400 [39]
$^{65}CuCl \rightarrow {}^{63}CuCl$	−0.076 [40]	3.220 [40]
$Cu^{37}Cl \rightarrow Cu^{35}Cl$	0.364 [41]	3.220 [41]
$Cd^{34}S \rightarrow Cd^{32}S$	0.370 [42]	2.580 [42]
$^{110}CdS \rightarrow {}^{116}CdS$	0.040 ÷ 0.068 [43]	2.580 [42]
$Cu_2^{18}O \rightarrow Cu_2^{16}O$	1.116 [44]	2.151 [44]
$^{71}GaAs \rightarrow {}^{69}GaAs$	0.39 [40]	1.53 [40]
$^{76}Ge \rightarrow {}^{72}Ge$	0.225 [42–47]	1.53 [42–47]
$^{76} \rightarrow {}^{73} \rightarrow {}^{70}Ge$	0.37 [46, 47]	0.74 [46, 47]

the *normal coordinates*, the Hamiltonian of our task will have the following relation (see, e.g. [26]):

$$H(Q, P) = \sum_{i,q} \left[-\frac{\hbar^2}{2} \frac{\partial^2}{\partial Q^2(\vec{q})} + \frac{1}{2}\omega_j^2 Q_j^2(\vec{q}) \right] \tag{1.9}$$

In this relation, the sum, where every addend means the Hamiltonian of linear harmonic oscillator with coordinate $Q_j(\vec{q})$, the frequency $\omega_j(\vec{q})$ and the mass equal a unit. If the Hamiltonian system consists of the sum, where every addend depends on the coordinate and conjugates its quasiimpuls, then according to quantum mechanics [48–50] the wave function of the system equals the product of wave functions of every appropriate addend and the energy is equal to the sum of assigned energies. Any separate term of the Hamiltonian (1.9) corresponds, as indicated above, with the *linear oscillator*

$$-\frac{\hbar^2}{2}\frac{\partial^2 \Psi}{\partial Q^2} + \frac{1}{2}\omega^2 Q^2 \Psi = \varepsilon \Psi. \tag{1.10}$$

Solving the last equation and finding the eigenvalues and eigenfunctions and then expressing explicitly the frequency, we will obtain for the model with two atoms in primitive cell (with masses M_1 and M_2; $M_1 > M_2$) the following equation:

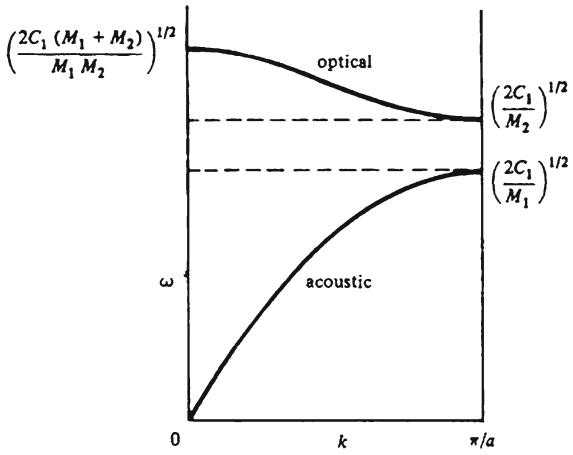

Fig. 1.2 Optical and acoustic modes. The optical modes lie at higher frequencies and show less dispersion than the acoustic modes (for details see text)

$$\omega^2 = \mathrm{C}\left(\frac{M_1+M_2}{M_1M_2}\right) \pm \left[\mathrm{C}^2\left(\frac{M_1+M_2}{M_1M_2}\right) - \frac{4C^2}{M_1M_2}\sin^2\frac{ka}{2}\right]$$

or

$$\omega_{\pm}^2 = \mathrm{A} \pm \left[\mathrm{A}^2 - \mathrm{B}\,\sin^2\frac{ka}{2}\right]^{1/2}. \tag{1.11}$$

There are now two solutions for ω^2, providing two distinctly separate groups of vibrational modes. The first group, associated with ω_-^2, contains the acoustic modes. The second group arises with ω_+^2 and contains the optical modes; these correspond to the movement of the different atom sorts in opposite directions (e.g. NaCl-structures), it is contra motion whereas the acoustic behavior is motion in unison.

For small ka we have from (1.11′) two roots:

$$\omega^2 \simeq 2\mathrm{C}\left(\frac{1}{M_1}+\frac{1}{M_2}\right)$$

and

$$\omega^2 \simeq \frac{\mathrm{C}}{2(M_1+M_2)}K^2a^2. \tag{1.12}$$

Taking into account that $K_{\max} = \pm\pi/a$, where a is a period of the crystal lattice, i.e., $K_{\max}$ respond to the border of the first *Brillouin zone* (see also Fig. 1.2)

$$\omega^2 = \frac{2\mathrm{C}}{M_1} \quad \text{and} \quad \omega^2 = \frac{2\mathrm{C}}{M_2} \tag{1.13}$$

As it is clear, formula (1.11′) describes the optical branch of vibrations whereas (1.12) the acoustical branch of vibrations. Usually the last formula is written as

follows:

$$\omega = \sqrt{\frac{\alpha}{M}}, \tag{1.14}$$

where α is the so-called force constant. Here, M is the mass of vibrated atom (ion). From the preceding relation it is clear that, as in molecular physics [21], in solids, the isotope effect directly manifests in vibration spectrum, which depends on the symmetry [30] measures either in IR—absorption or in *Raman scattering* of light. Before analyzing Raman scattering spectra of different solids we briefly consider the classical approximation of the mechanism of Raman effect [51–53].

Historically, Raman scattering denotes inelastic scattering of light by molecular vibrations or by optical phonons in solids. In a macroscopic picture, the Raman effect in crystals is explained in terms of the modulation of polarizability by the quasiparticle under consideration. The assumption that the polarization depends linearly upon the electric field strength [54] is a good approximation and is invariably used when discussing the scattering of light by crystal excited by lasers. However, the approximation is not valid for large strength such as can be obtained from pulsed lasers [55]. The polarization may then be expressed as

$$P = \alpha \mathrm{E} + \frac{1}{2}\beta \mathrm{E}^2 + \frac{1}{6}\gamma \mathrm{E}^3 + \frac{1}{24}\delta \mathrm{E}^4 + \ldots\ldots, \tag{1.15}$$

where β, the first hyperpolarizability coefficient, plays an important part for large values of E, since it is responsible for the phenomenon of optical harmonic generation using Q-switched lasers. Isolated atoms have $\beta = 0$, since, like μ the dipole moment, it arises from interactions between atoms. A simplified theory of Rayleigh scattering, the *Raman effect*, harmonic generation and hyper Raman scattering is obtained by setting (see, e.g. [55])

$$\mathrm{E} = \mathrm{E}_0 \cos \omega_0 \mathrm{t}, \tag{1.16}$$

$$\alpha = \alpha_0 + \left(\frac{\partial \alpha}{\partial Q}\right) Q, \tag{1.17}$$

$$\beta = \beta_0 + \left(\frac{\partial \beta}{\partial Q}\right) Q, \tag{1.18}$$

$$Q = Q_0 + \cos \omega_v \mathrm{t}. \tag{1.19}$$

Here, Q is a normal coordinate, ω_v is the corresponding vibrational frequency and ω_0 is the laser frequency. After that we have

$$\mathrm{P} = \alpha_0 \mathrm{E}_0 \cos\omega_v t + \frac{1}{2}\left(\frac{\partial\alpha}{\partial Q}\right) Q_0 \mathrm{E}_0 \cos\omega_0 \mathrm{t}\cos\omega_v t + \frac{1}{2}\beta_0 \mathrm{E}_0^2 \cos^2\omega_0 t + \frac{1}{2}\left(\frac{\partial\beta}{\partial Q}\right) \mathrm{Q}_0 \mathrm{E}_0^2 \cos^2\omega_0 \mathrm{t}\cos\omega_v t. \tag{1.20}$$

Then, after small algebra, we obtain

$$\mathrm{P} = \alpha_0 \mathrm{E}_0^2 \cos\omega_v t + \frac{1}{2}\left(\frac{\partial\alpha}{\partial Q}\right) Q_0 \mathrm{E}_0 \cos(\omega_0 - \omega_v)t + \cos(\omega_0 + \omega_v)t + \frac{1}{2}\beta_0 \mathrm{E}_0^2 + \frac{\beta_0}{4}\mathrm{E}_0^2 \cos\,2\omega_0 t + \frac{1}{2} Q_0 \mathrm{E}_0^2 \left(\frac{\partial\beta}{\partial \mathrm{Q}}\right) \cos(2\omega_0 - \omega_v)t + \cos(2\omega_0 - \omega_v)t. \tag{1.21}$$

In the last relation the first term describes the Rayleigh scattering, second—*Raman scattering*, third—d.c. polarization, fourth—frequency doubling and the last—hyper Raman effect. Thus the hyper Raman effect is observed with large electric field strength in the vicinity of twice the frequency of the exciting line with separations corresponding to the vibrational frequencies. α and β are actually tensors and β components $\beta_{\alpha\beta\gamma}$ which are symmetrical suffixes [30].

Semiconducting crystals (C, Si, Ge, $\alpha - \mathrm{Sn}$) with diamond-type structure present ideal objects for studying the isotope effect by the Raman light-scattering method. At present, this is facilitated by the availability of high-quality crystals grown from isotopically enriched materials (see, e.g [56] and references therein). In this part our understanding of first-order Raman light scattering spectra in isotopically mixed elementary and compound (CuCl, GaN, GaAs) semiconductors having a zinc blende structure is described. Isotope effect in light scattering spectra in Ge crystals was first investigated by Agekyan et al. [57]. A more detailed study of Raman light scattering spectra in isotopically mixed Ge crystals has been performed by Cardona and Thewalt [56].

It is known that materials having a diamond structure are characterized by the triply degenerate phonon states in the Γ point of the *Brillouin zone* ($\vec{k} = 0$). These phonons are active in the Raman scattering spectra, but not in the IR absorption one [51]. Figure 1.3a demonstrates the dependence of the shape and position of the first-order line of optical phonons in germanium crystal on the isotope composition at liquid nitrogen temperature (LNT) [58]. The coordinate of the center of the scattering line is proportional to the square root of the reduced mass of the unit cell, i.e., $\sqrt{M}$. It is precisely this dependence that is expected in the harmonic approximation. An additional frequency shift of the line is observed for the natural and enriched germanium specimens and is equal, as shown in Ref. [56] to 0.34 ± 0.04 and $1.06 \pm 0.04\,\mathrm{cm}^{-1}$, respectively (see, e.g. Fig. 4.7 in Chap. 4 of Ref. [59]).

First-order Raman light-scattering spectrum in diamond crystals also includes one line with maximum at $\omega_{\mathrm{LTO}}(\Gamma) = 1,332.5\,\mathrm{cm}^{-1}$. In Fig. 1.3b the first-order scattering spectrum in diamond crystals with different isotope concentrations is shown [60]. As shown below, the maximum and the width of the first-order scattering line in

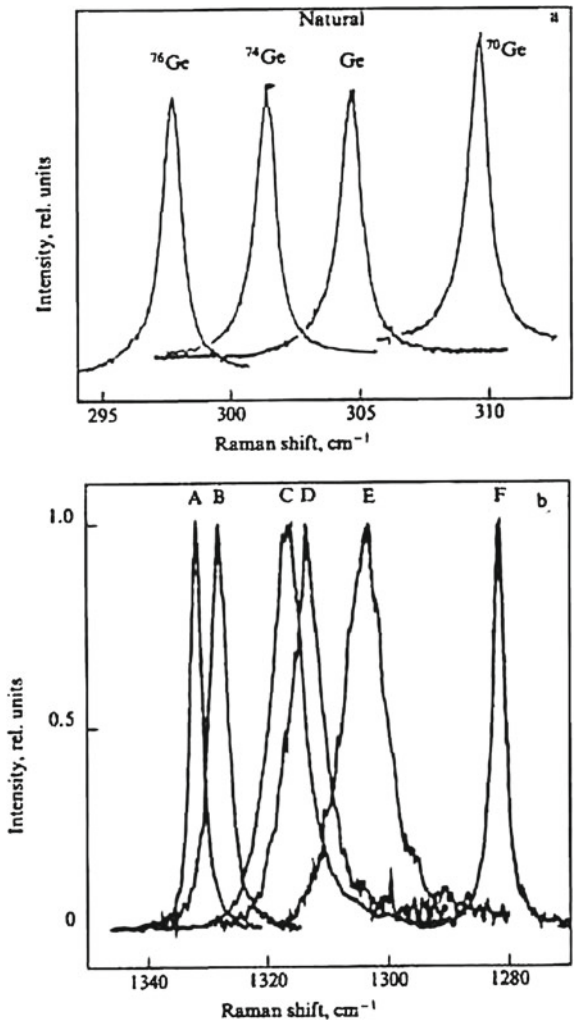

Fig. 1.3 **a** First-order Raman scattering spectra Ge with different isotope contents [56] and **b** First-order Raman scattering in isotopically mixed diamond crystals $^{12}C_x^{13}C_{1-x}$. The peaks A, B, C, D, E and F correspond to $x = 0.989$; 0.90; 0.60; 0.50; 0.30 and 0.001 (after [60])

isotopically mixed diamond crystals are nonlinearly dependent on the concentration of isotopes x. The maximum shift of this line is 52.3 cm^{-1}, corresponding to the two limiting values of $x = 0$ and $x = 1$. Analogous structures of first-order light scattering spectra and their dependence on isotope composition has by now been observed many times, not only in elementary Si and $\alpha - Sn$, but also in compound CuCl and GaN semiconductors (for more details see reviews [31, 56]). Already a shortlist of data shows a large dependence of the structure of first-order light-scattering spectra in diamond as compared to other crystals (Si, Ge). This is the subject of detailed discussion in [61].

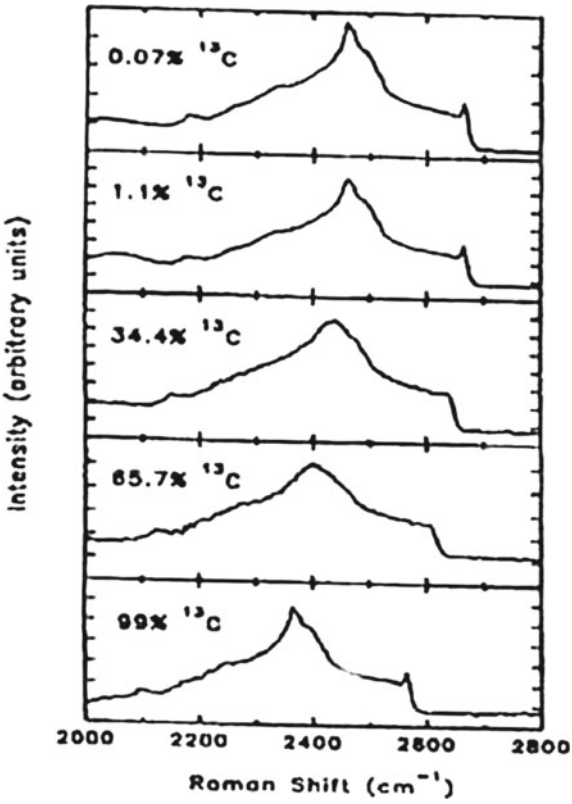

Fig. 1.4 Second-order Raman scattering spectra in synthetic diamond with different isotope concentration at room temperature (after [63])

Second-order Raman spectra in natural and isotopically mixed *diamonds* have been studied by Chrenko [62] and Hass et al. [63]. Second-order Raman spectra in a number of synthetic diamond crystals with different isotope compositions shown in Fig. 1.4 are measured wit resolution ($\sim 4\,\mathrm{cm}^{-1}$) worse than for first-order scattering spectra. The authors of the cited work explain this fact by the weak signal in the measurement of second-order Raman scattering spectra. It is appropriate to note that the results obtained in [63] for natural diamond ($C_{13_C} = 1.1\%$), agree well with the preceding comprehensive studies of Raman light-scattering spectra in natural diamond [64]. As is clearly seen from Fig. 1.4 the structure of second-order light scattering "follows" the concentration of the ^{13}C *isotope*. It is necessary to add that in the paper by Chrenko [64] one observes a distinct small narrow peak above the high-frequency edge of LO phonons and the concentration of ^{13}C x = 68%. Note in passing that second-order spectra in isotopically mixed diamond crystals were measured in the work by Chrenko [62] with a better resolution than the spectra shown in Fig. 1.4. Second-order Raman light scattering spectra and IR absorption spectra in crystals of natural and isotopically enriched ^{70}Ge can be found in [31].

A comprehensive interpretation of the whole structure of second-order Raman light-scattering spectra in pure LIH (LiD) crystals is given in [22, 61]. Leaving this question, let us now analyze the behavior of the highest frequency peak after the substitution of hydrogen for deuterium (see, also [65]).

Absorption behavior of an IR-active phonon in mixed crystals with a change in the concentrations of the components can be classified into two main types: one and two-mode (see, e.g. the review [66]). *Single-mode behavior* means that one always has a band in the spectrum with a maximum gradually drifting from one endpoint to another. *Two-mode behavior* is defined by the presence, in the spectrum, of two bands characteristic of each components leading not only to changes in the frequencies of their maxima, but mainly to a redistribution of their intensities. In principle, one and the same system can show different types of behavior at opposite ends [67]. The described classification is qualitative and is rarely realized in its pure form (see, also [67]). The most important necessary condition for the two-mode behavior of phonons (as well as of electrons [68]) is considered to be the appearance of the localized vibration in the localized defect limit. In the review [66] a simple qualitative criterion for determining the type of the IR *absorption behavior* in crystals with an NaCl structure type has been proposed (see also [68]). Since the square of the TO (Γ) phonon frequency is proportional to the reduced mass of the unit cell M, the shift caused by the defect is equal to

$$\Delta = \omega_{\mathrm{TO}}^2 \left(1 - \frac{\overline{\mathrm{M}}}{\overline{\mathrm{M}}'}\right). \tag{1.22}$$

This quantity is compared in [66] with the width of the optical band of phonons which, neglecting acoustical branches and using the parabolic dispersion approximation, is written as

$$W = \omega_{\mathrm{TO}}^2 \left(\frac{\varepsilon_0 - \varepsilon_\infty}{\varepsilon_0 + \varepsilon_\infty}\right). \tag{1.23}$$

A local or gap vibration appears, provided the condition $|\Delta| > (1/2)W$ is fulfilled. As mentioned, however, in [66] in order for the two peaks to exist up to concentrations of the order of $\sim$0.5, a stronger condition $|\Delta| > W$ has to met. Substituting the numerical values from Table 1.1 of [61] into formulas (1.22) and (1.23) shows that for LiH (LiD) there holds (since $\Delta = 0.44\,\omega_{\mathrm{TO}}^2$ and $W = 0.58\omega_{\mathrm{TO}}^2$) the following relation:

$$|\Delta| > (1/2)W. \tag{1.24}$$

Thereby, it follows that at small concentrations the local vibration should be observed. This conclusion is in perfect agreement with earlier described experimental data [65]. As to the second theoretical relation $\Delta > W$, one can see from the above discussion that for LiH (LiD) crystals the opposite relation, i.e., $W > \Delta$, is observed [20].

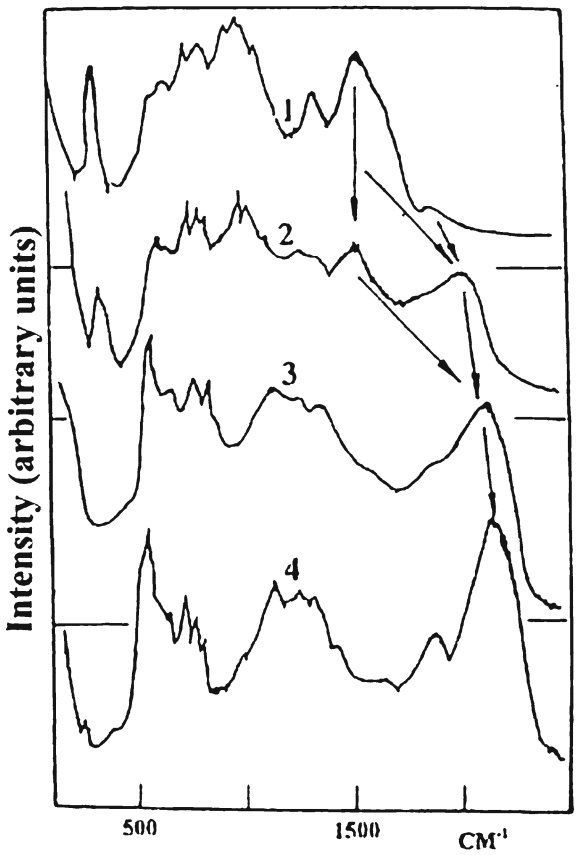

Fig. 1.5 Second-order Raman scattering spectra in the isotopically mixed crystals LiH_xD_{1-x} at room temperature. $1 - x = 0; 2 - 0.42; 3 - 0.76; 4 - 1$. The *arrows* point out a shift of LO(Γ) phonons in the mixed crystals (after [61])

Following the results of [69], in Fig. 1.5 we show the second-order Raman scattering spectra in mixed LiH_xD_{1-x} crystals at room temperature. In addition to what has been said on Raman scattering spectra at high concentration [69], we note that as the concentration grows further ($x > 0.15$) one observes in the spectra a decreasing intensity in the maximum of 2LO (Γ) phonons in LiD crystal with a simultaneous growth in intensity of the highest frequency peak in mixed LiH_xD_{1-x} crystals. The nature of the latter is in the renormalization of LO(Γ) vibrations in mixed crystal [70]. Comparison of the structure of Raman scattering spectra (curves 1 and 2 in Fig. 1.5) allows us, therefore, to conclude that in the concentration range of $0.1 < x < 0.45$ the Raman scattering spectra simultaneously contain peaks of the LO(Γ) phonon of pure LiD and the LO(Γ) phonon of the mixed $LiH_xD1 - x$ crystal. For further concentration growth ($x > 0.45$) one could mention two effects in the Raman scattering spectra of mixed crystals. The first is related to an essential reconstruction of the acoustooptical part of the spectrum. This straightforwardly follows from a comparison of the structure of curves 1–3 in Fig. 1.5. The second effect originates from a further shift of the highest frequency peak toward still higher frequencies, related to

the excitation of LO(Γ) phonons. The limit of this shift is the spectral location of the highest frequency peak in LiH. Finishing our description of the Raman scattering spectra, it is necessary to note that a resonance intensity growth of the highest frequency peak is observed at $x > 0.15$ in all mixed crystals (for more details see [72]).

One more reason for the discrepancy between theory and results of the experiment may be connected with not taking into account in theory the change of the *force-constant* at the *isotope substitution* of the smaller in size D by H ion [72]. We should stress once more that among the various possible isotope substitutions, by far the most important in vibrational spectroscopy is the substitution of hydrogen by deuterium. As is well known, in the limit of the Born-Oppenheimer approximation the force-constant calculated at the minimum of the total energy depends upon the electronic structure and not upon the mass of the atoms. It is usually assumed that the theoretical values of the phonon frequencies depend upon the force-constants determined at the minimum of the adiabatic potential energy surface. This leads to a theoretical ratio $\omega\,(\mathrm{H})\,/\omega\,(\mathrm{D})$ of the phonon frequencies that always exceed the experimental data. Very often anharmonicity has been proposed to be responsible for a lower value of this ratio. In isotope effect two different species of the same atom will have different vibrational frequencies only because of the difference in isotopic masses.

http://www.springer.com/978-3-642-28612-4

Isotope Low-Dimensional Structures
Elementary Excitations and Applications
Plekhanov, V.G.
2012, XII, 96 p. 51 illus., Softcover
ISBN: 978-3-642-28612-4